

Flux generation and sustainment of a field reversed configuration with rotating magnetic field current drive*

J. T. Slough[†] and K. E. Miller

Redmond Plasma Physics Laboratory, University of Washington, Seattle, Washington 98195

(Received 19 November 1999; accepted 7 February 2000)

A new experimental device has been constructed to study the flux build-up and sustainment of a field reversed configuration (FRC) with a rotating magnetic field (RMF). Even though complete penetration was expected from RMF theory, the RMF field was observed to penetrate only a few centimeters inside the FRC separatrix. Despite the limited penetration, significantly larger toroidal currents (40 kA) were driven than in previous experiments (~ 2 kA) with the same RMF field. The high currents and lack of deep penetration allowed the axial field to be the dominant field throughout the FRC. The radially inward ponderomotive force arising from axial screening currents at the FRC edge had a significant influence on energy and particle confinement, reducing convective losses to the limit of observability. With only ohmic heating, the measured low ion temperatures (2 eV) left the ions unmagnetized while the electrons (~ 40 eV) were well magnetized. No destructive instability was observed for the RMF driven FRC despite the lack of a strong kinetic ion component.

© 2000 American Institute of Physics. [S1070-664X(00)96305-5]

I. INTRODUCTION

Fusion research in recent years has focused on the tokamak concept which, while reaching near break-even thermonuclear conditions, has resulted in large, expensive reactor designs. This dictates exploring novel, simpler and less costly configurations. A leading candidate is the field-reversed configuration (FRC), a compact toroidal geometry, which is the geometrically simplest, most compact, and highest power density of all currently studied magnetic fusion confinement schemes.¹ It has also been recognized that the linear geometry, high plasma pressure, and linear exhaust of the FRC make it the ideal candidate for space propulsion applications.²

FRCs are presently made in a high voltage pulsed device called a field-reversed theta pinch (FRTF). Even though the results from the largest FRC experiment to date indicated confinement scaling adequate for fusion,³ it was also clear that the FRTF initiation method could not provide the required confining closed flux into the reactor regime. There is a method that has been investigated experimentally for years that generates the toroidal currents directly by means of a transverse rotating magnetic field (RMF) as illustrated in Fig. 1.⁴⁻⁶ Past experiments have been limited to currents of only a few kiloamps, so that the confining axial magnetic field generated, B_e , was no larger than the rotating field B_ω . The effects of the RMF on the FRC plasma confinement were also unknown as the plasmas generated in these experiments were partially ionized and in contact with the vessel wall.

A new experiment, the Star Thrust Experiment (STX),² was constructed at the University of Washington of a size and power such that the axial field swing ΔB_z (200 G), produced by the RMF field, was much larger than the RMF field

B_ω (20 G) used to generate it. The FRC was also formed in a flux conserving coil and operated in a manner that prevented FRC plasma contact with the vacuum vessel wall. STX was also equipped with diagnostics that shed light on the effect of the RMF on confinement as well.

STX was designed so that the FRC could be produced in the conventional manner, i.e., by rapid field reversal in a field reversed theta pinch coil (FRTF). In this way, the possibility of sustaining a preexisting FRC could also be investigated, as well as obtaining a measure of the influence of the RMF on the decaying FRC. It was also possible to form the FRC with the RMF alone, using the fast field reversal only for preionization.

The paper is arranged into the following sections. The second section will give a brief review of the physics relevant to RMF penetration. This will be followed by a description of the STX experiment. Results from experiments will be presented in the fourth section. Based on the results, a discussion of future directions will be presented in the final section.

II. RMF THEORY

When applied to a plasma embedded with a constant axial magnetic field in a flux conserving coil, the RMF drives a strong azimuthal current that reverses the direction of the initial magnetic field, and produces the field reversed configuration (see Fig. 1). Unlike FRTF formation, where this current is driven by an induced azimuthal voltage caused by a rapid reversal of the external field, the RMF current is driven in an inherently steady state manner which allows for the sustainment of the configuration. A starting point for understanding the current drive process is the generalized Ohm's Law,

$$\mathbf{E} = \eta \mathbf{j} + \mathbf{j} \times \mathbf{B} / ne = \eta [\mathbf{j} + (\omega_{ce} / \nu_{ei}) \mathbf{j} \times \mathbf{e}_b], \quad (1)$$

*Paper D111 Bull. Am. Phys. Soc. **44**, 84 (1999).

[†]Invited speaker.

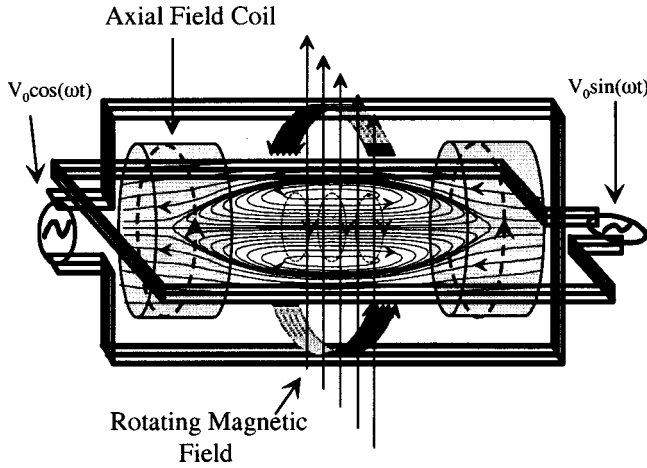


FIG. 1. RMF current drive in a cylindrical flux-conserving coil.

where B has oscillating components in the θ and r directions (B_θ, B_r) due to the RMF at a frequency ω_{RMF} , and a steady axial field provided by the axial field coils (see Fig. 1). If the Hall term $\mathbf{j} \times \mathbf{B}/ne$ is small compared to the resistive term, $E_\theta = \eta j_\theta$ is positive, and from Faraday's law, $d\phi/dt$ is negative. This means poloidal flux is leaving the FRC (less field reversal) and it is decaying. With the Hall term included, E_θ , for sufficiently small η or large $j_z B_r$, can be negative. The axial current is driven by an induced axial electric field, and the Hall term has the opposite sign of ηj_θ . When E_θ is negative, $d\phi/dt$ is positive, flux is entering the FRC, and it is growing (more field reversal). In the fluid picture, the RMF field induces an oscillatory $E_z = \omega r B_r \cos(\omega t)$ which drives an oscillatory j_z such that the steady component of $\langle j_z B_r \rangle$ produces an azimuthal force that opposes the ohmic ηj_θ . In the particle picture, the electrons are magnetized in the RMF and rotate cosynchronously with it, while the much more massive ions remain unmagnetized.

A requirement on the RMF is then that the electrons stay magnetized while the ions are not,

$$v_{ei} \ll \omega_{ce}, \quad (2a)$$

$$\omega_{ci} < \omega_{\text{RMF}} < \omega_{ce}. \quad (2b)$$

The first part of this requirement is obvious from the extended form of Eq. (1), if the Hall term is to dominate over the resistive term. The condition on the RMF rotational frequency assures that the ions do not also corotate with the RMF, as this would eliminate the current drive. Even if the ions are not magnetized in the RMF field, it is also necessary that the electrons do not transfer their momentum to the ions over a long time scale. Two-fluid calculations show this is achieved with minimal fueling rates since the fuel ions are deposited with zero angular momentum, and they diffuse out faster than they gain momentum from collisions with the electrons.

The second requirement on the RMF is that it penetrate the plasma. The RMF effective skin depth should be on the order of the FRC's radius. The solution of Ohm's law, neglecting the Hall term, is characterized by the RMF penetrating a distance $\delta = (2\eta/\omega\mu_0)^{1/2}$, which is the resistive skin

depth for a conductor in an RF field. The regime of interest, however, is that of a hot, low resistivity plasma with $v_{ei} \ll \omega_{ce}$. In this regime, the Hall term dominates and the solution to Ohm's law yields $j_\theta \approx ner\omega$ and $j_z \approx E_z/(\eta\omega_{ce}^2/2v_{ei}^2)$, which implies that the electrons are in synchronous rotation with the RMF and that their axial oscillation is severely restricted. This suggests an effective resistivity of $\eta_{\text{eff}} = \eta\omega_{ce}^2/2v_{ei}^2$, and an effective skin depth of $\delta_{\text{eff}} = (\omega_{ce}/v_{ei})\delta$.

One can then define two dimensionless parameters that describe the RMF penetration condition,

$$\gamma_\omega = \omega_{ce}/v_{ei}, \quad \lambda = R/\delta, \quad (3a)$$

where

$$\gamma_\omega = \left(\frac{B_\omega}{en\eta} \right) \quad \lambda = \left(\frac{\omega\mu_0}{2\eta} \right)^{1/2} R. \quad (3b)$$

Penetration can be maintained as long as $\gamma_\omega > \lambda$.^{7,8}

The inferred STX electron temperature from pressure balance was $T_e \sim 40$ eV. The experiments were performed at an RMF frequency $\omega = 2.2 \times 10^6$ rad/sec, and at an average RMF vacuum field $B_\omega = 20$ Gauss. The density at a radius of 15 cm was found from axial interferometry to be $\sim 5 \times 10^{18} \text{ m}^{-3}$. These conditions imply a $\lambda \approx 65$, with a $\gamma_\omega = 375$. These values are well above critical and the RMF field would be expected to fully penetrate the plasma.

It should be noted that the Hall term has two components: the $\langle j_z B_r \rangle$ term acting in the θ direction, and $\langle j_z B_\theta \rangle$ term acting in the r direction. It should also be noted that since j_z , B_r , and B_θ vary in time at the frequency ω_{RMF} , the ponderomotive forces in θ and r directions have both a steady part and an oscillatory part at a frequency of $2\omega_{\text{RMF}}$. Due to the effect of the first $\langle j_z B_r \rangle$ force, the electron fluid will attain that steady value of azimuthal velocity, $v_{e\theta}$, that corresponds to the balancing of the steady accelerating torque by the retarding torque (due to the collisions of the electrons with the ions). In this way a steady azimuthal current density,

$$j_\theta = -ne\omega_{\text{RMF}}r, \quad (4)$$

is produced.

Now consider the effect of the second, radially acting $\langle j_z B_\theta \rangle$ force. When it acts on the electron fluid, a counter-acting radial electrostatic field is produced which stops the flow of radial current, as is the usual response of a conductor when the Hall effect is significant. This radial force was found to be quite significant in the experiment as it provided a confining force that inhibited the radial diffusion of plasma.

III. THE STX EXPERIMENT

The STX vacuum wall consists of a 3-m long, 40-cm diameter quartz plasma tube that is surrounded by four turn solenoidal coils to provide an axial confinement field. Special "half" turn antennas, described below, produce the rotating magnetic field. A schematic of the device is shown in Fig. 2.

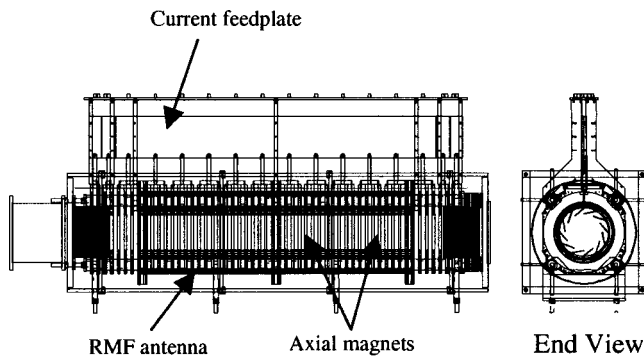


FIG. 2. Schematic of the STX device. RMF antenna length was 2 m.

The RMF is generated by two mutually perpendicular coils running the length of the experiment and driven 90 deg out of phase. To satisfy field uniformity constraints, each antenna coil is separated into two parallel coils, where the coil separation is set by a Helmholtz-like minimization to be R when the wires are at radius R from the axis of the machine. The antennas are placed outside the confinement coils, at $R=36$ cm. The large radius provides for greater field uniformity inside the 20-cm plasma tube radius and minimizes the higher harmonic content in the RMF. The contamination from higher harmonics was found to be detrimental to RMF penetration in numerical analysis of the RMF current drive near the RMF antennas.⁷

In order to drive the RMF antennas, the two power supplies were capable of delivering several megawatts for the duration of the experiment in order to rapidly ionize the plasma and heat the electrons to a temperature such that the $\omega_{ce} \gg \nu_{ei}$ is satisfied. The antenna power was provided by a resonant tank circuit driven by Isolated Gate Bipolar Transistor (IGBT) switches which are very high current on-off solid state devices. Each of two power supplies employs 12 IGBTs in parallel, with a primary current on the order of 12 kA. This current passes through the primary of a 20:1 air core transformer, the secondary of which forms a parallel LC tank circuit ($Q \sim 60$), where the inductor is the RMF antenna. The tank circuit high Q transforms the square wave nature of the switch into a sinusoid. The parallel tuned circuit holds the voltage on the antenna constant, so that as the plasma load increases, more current is drawn from the supply with minimal drop in antenna field. A schematic of the RMF driver system is shown in Fig. 3. The resulting RMF field wave form during a plasma discharge is shown in Fig. 4. The RMF frequency was 350 kHz for these experiments. The filling gas for all results presented was deuterium. The RMF driven FRC discharge was initiated as the neutral gas was pumped away from and original static fill of 20 mTorr. This was done to allow for a glow discharge to be initiated at high fill pressure, and then to be maintained down to very low filling pressures desired for the experiments. The fill pressure was estimated to be less than 0.3 mTorr at the time of FRC initiation ($t=0$ in all plots).

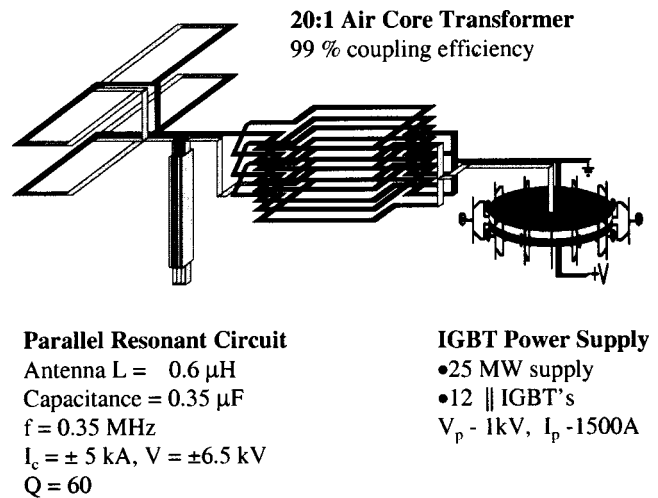


FIG. 3. RMF antenna driver system.

IV. EXPERIMENTAL RESULTS

STX was equipped with a bank that allowed for the fast reversal of the axial magnetic field. With the ability to form an FRC independent of the RMF, several modes of FRC formation and sustainment could be examined experimentally. Due to the pulse nature of the power supplies, the time that the flux could be held constant on the main pinch coil was limited to roughly 0.5 ms (see Fig. 4). This, however, was sufficient to establish an equilibrium condition and gain information about the power input and losses from the FRC. From Fig. 4 it can be seen that the FRC separatrix radius,

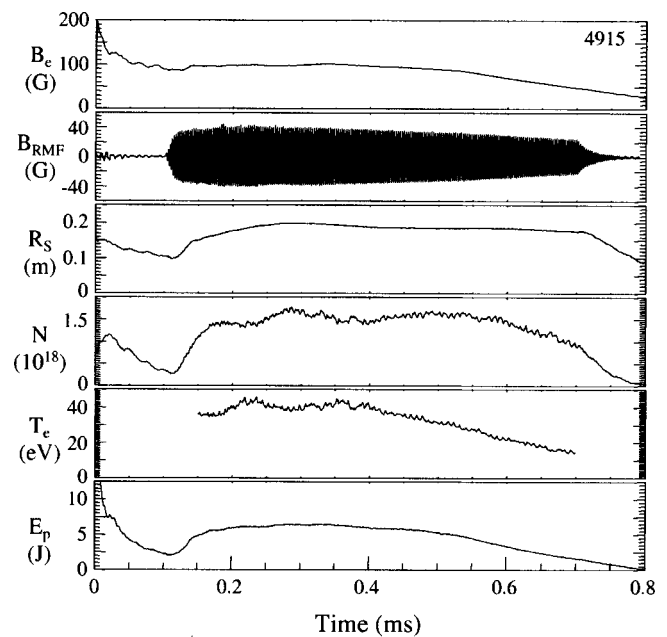


FIG. 4. Time history for various plasma parameters during a discharge where a FRTP FRC is produced at $t=0$. B_e is the external axial field at the axial midplane, B_{RMF} is the magnitude of the θ component of the RMF at the wall radius ($r=20$ cm), R_s is the FRC separatrix radius, N is the FRC particle inventory, T_e is the electron temperature, and E_p is the FRC total plasma energy.

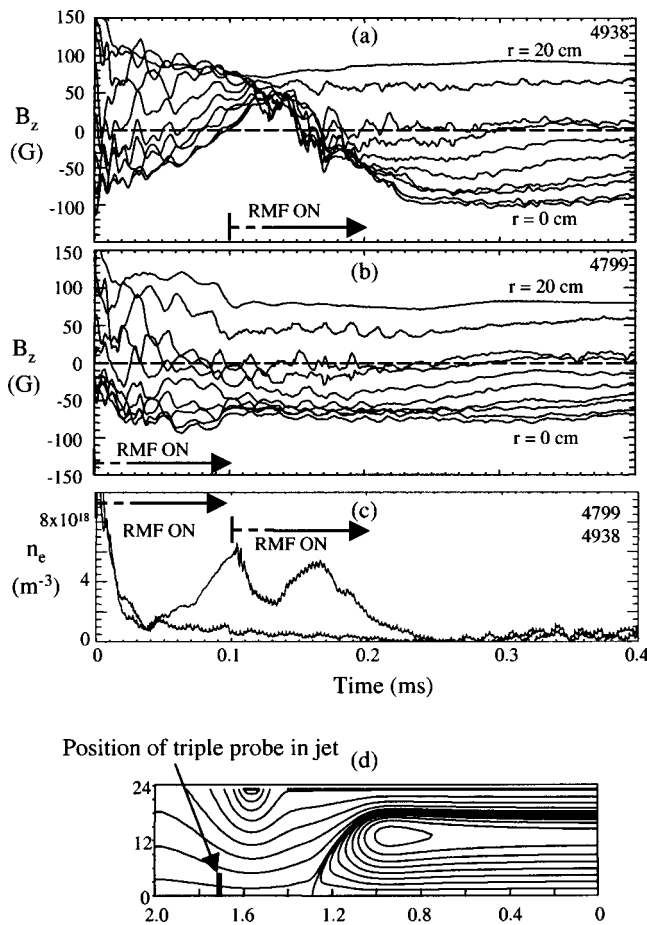


FIG. 5. Time history of the axial magnetic field at various radii from the internal magnetic probe. The probes were separated by roughly 2 cm radially. (a) Magnetic traces for a discharge where the RMF was turned on at 0.1 ms. (b) Magnetic traces for a discharge where the RMF was turned on at $t=0$. (c) Time history of the density determined by a triple probe in the end region of STX for the discharges in (a) and (b). (d) Magnetic field geometry from a two-dimensional numerical FRC calculation for the axial fields employed in (a) and (b).

energy and particle inventory remain essentially constant during the time the coil flux could be held constant.

The formation sequence employed in the discharge shown in Fig. 4 was to first form an FRC via the FRTP method. As can be seen in Fig. 4, the initial FRC decays away rapidly. Out of the remnant plasma, the RMF was turned on at 0.1 ms and even more rapidly restores the toroidal current and re-forms the FRC. A plot of the internal field structure from the inner wall of the STX vacuum chamber at $r=20$ cm to the axis of symmetry ($r=0$) is shown in Fig. 5(a). These data were obtained from a radial array of internal magnetic probes' array that recorded both the axial and azimuthal internal field components. It can be seen that there are large fluctuations in the axial field during the decay of the initial non-RMF FRC. After field reversal is reestablished, little of this magnetohydrodynamic (MHD) activity is observed. In Fig. 5(b) the RMF is applied immediately after field reversal. In this case the initial FRC turbulence dies away and field reversal is never lost. A Langmuir triple probe was used to monitor the plasma flow in the end region axially outside the FRC as shown in Figs. 5(c) and 5(d).

From this probe the end flow increases steadily during the decay of the initial FRTP FRC. It is not until the RMF FRC is established that the end flow is reduced to near zero. For the case where there is RMF from the initiation of field reversal, the flow is significantly reduced from the start. From this and other analysis given elsewhere,⁹ it is believed that the FRC stability and particle confinement are dramatically improved by the presence of the RMF fields at the FRC separatrix. Although previous RMF experiments were operated for 100 s of Alfvén times, these experiments were unable to determine the quality of confinement due to wall contact. Basic plasma stability was also unknown since the observed gross stability could be due to either wall stabilization or continual regeneration of the magnetic structure.¹⁰

From previous analysis,^{7,11} the RMF must diffuse radially inward into the FRC in order to drive current. The time scale for penetration into conducting cylindrical plasma of radius R is roughly given by

$$\tau_{\text{pen}} \sim \frac{1}{8} \mu_0 \frac{R^2}{\eta}.$$

Using the equilibrium values for the RMF FRC, $\tau_{\text{pen}} \sim 0.7$ ms. The actual ramp-up time could be made as short as 0.05 ms, indicating that the resistivity of the decaying FRC is much greater than classical at 40 eV. Langmuir triple probe data indicate that the electron temperature is ~ 15 eV in the initial FRTP FRC, but even at that temperature an anomalous factor is still inferred. After the RMF FRC is formed, if the RMF field is separated from the FRC, re-penetration is not observed, indicating the resistivity near the FRC separatrix is much lower. The inferred resistivity during the time of RMF FRC sustainment from power balance considerations between the antenna input power and the FRC resistive dissipation was found to be near classical.⁹

The evolution of the magnetic profile during the equilibrium period is shown in Fig. 6. It can be seen that the current density profile is initially close to the linear function of radius that would be expected from Eq. (4). The FRC current profile after the initial flux build-up shows a steady evolution to a thin flux layer profile with little current being driven near the magnetic null. The ohmic heating of the plasma is seen to occur primarily near the FRC edge (Fig. 6). The electron temperature is thus assumed to be constant throughout the FRC at the temperature inferred from the interferometer at $r=15$ cm. The internal flux is also observed to slowly decay.

This process of rapid current ramp-up and then subsequent slow decay is a natural consequence of the RMF current drive process in a flux conserving shell. As illustrated in Fig. 7, the increasing flux produces a larger radius FRC that places the electron current sheath further out radially. The electron azimuthal velocity at the new larger radius is less than cosynchronous. The RMF brings these electrons up to the synchronous velocity $v_{e\theta} = \omega r$. This increases the total driven current that then produces more flux, which in turn increases the FRC radius. Eventually, the rising external field produced by the increasing flux halts the radial (and flux) increase. Experimentally the FRC separatrix radius increases

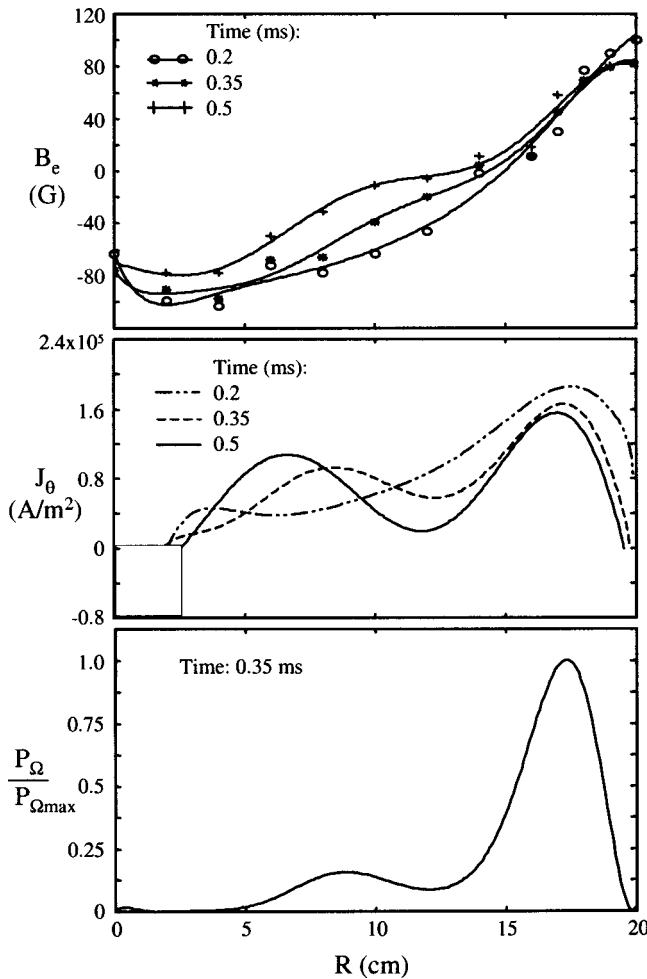


FIG. 6. Axial magnetic field profiles at various times during an RMF discharge. The current profiles are derived from an 8th order polynomial fit to the magnetic profile data. P_{Ω} is the ohmic power dissipated in the FRC assuming a uniform electron temperature.

until it is at roughly the wall radius of 20 cm. The external field at this point has risen to about three times its vacuum value before the expansion is halted. The inevitable rebound of this motion sets in place a ramp-down of the FRC flux for exactly the same reasons the flux was increased. But here, there is little to halt the process, although a carefully controlled decrease in coil flux allowed the FRC separatrix to remain nearly constant, and the decay rate to be much slower than the ramp-up (see Fig. 4). In future experiments it will be

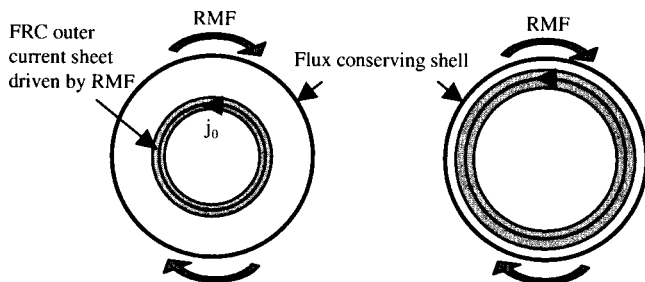


FIG. 7. FRC radial dynamics from RMF current ramp-up (and down).

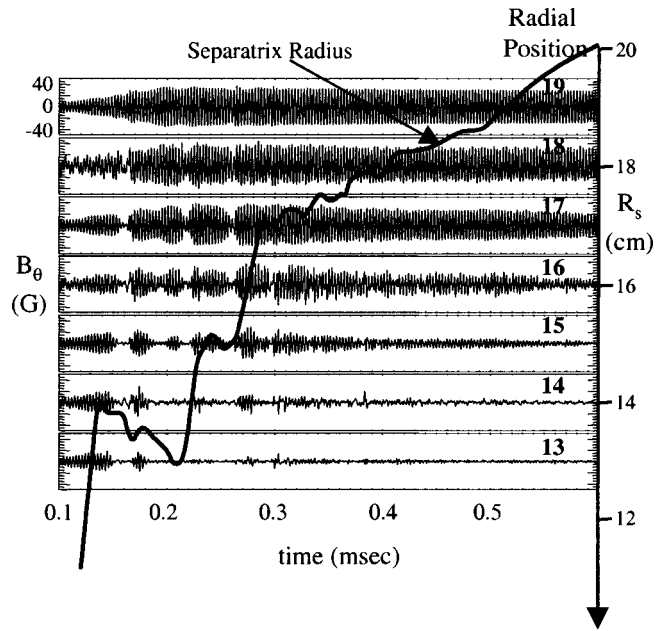


FIG. 8. Temporal traces of the θ component of the RMF at different radii. Superimposed on traces is a plot of the FRC separatrix radius measured by the external excluded flux array.

important to be able to control the external flux on the coil in order to prevent this “bounce” dynamic.

By starting with a sufficiently low filling pressure (~ 0.2 mTorr D_2), it was possible to have no initial FRC and start the FRC from just a partially preionized plasma. Again by careful manipulation of the external field decay, it was possible to stay in the constantly increasing flux mode throughout the entire discharge pulse. A plot of the FRC separatrix during this prolonged ramp-up can be found in Fig. 8. Also onto this figure are plotted the traces of the amplitude of the θ component of the RMF field at various radii measured by the internal probe. Quite surprisingly, it can be seen that the RMF field is screened from all but the outer few centimeters near the FRC separatrix during the entire flux build-up. The lack of significant RMF penetration is characteristic of the ramp-down phase as well. The magnitude of the RMF field in vacuum was ~ 20 G. It can be seen in both Figs. 4 and 8 that the measured θ component is twice that, which would be expected from the complete screening of the RMF by the plasma. The thickness of the axial current sheath is on the order of the probe resolution, ~ 1 cm.

Clearly, deep penetration of the FRC is not required to drive current and reverse the axial magnetic field deep within the FRC. How this is possible is not fully understood, but it is most likely a result of the axial equilibrium constraints that come into play when sufficient edge current is driven to reduce the inner axial field to near zero.

A major consequence of the peripheral penetration is that the radial pondermotive term, $\langle j_z B_{\theta} \rangle$, is increased by the screening currents. In previous work it was recognized that this radial force was a confining force.¹² In STX, the rapid attenuation of the RMF fields near the separatrix resulted in a large reduction in the plasma density at the FRC separatrix,

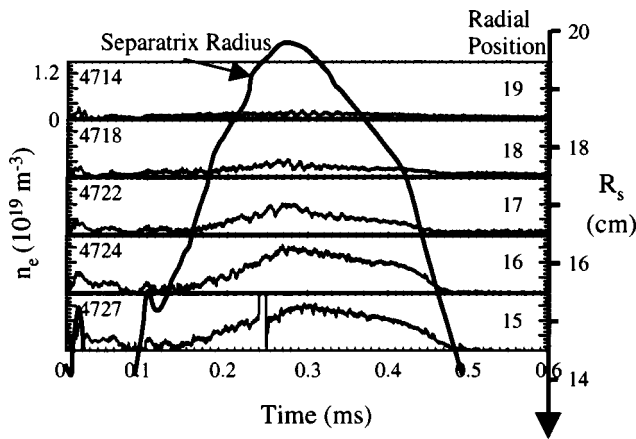


FIG. 9. Temporal traces of density from the triple probe at different radii. Superimposed on traces is a plot of the FRC separatrix radius measured by the external excluded flux array.

as the plasma was swept inward. In Fig. 9 a plot of the FRC separatrix radius determined from the external array of excluded loops is again superimposed on traces of density obtained from the triple probe at various radii near the vacuum wall. It can be seen that during the entire expansion (and, for that matter, contraction) of the FRC separatrix radius that the separatrix density is kept quite low. This is primarily why having the FRC separatrix close to (and even outside of) the wall did not cause significant energy loss or impurity increase.

Conventional FRTP FRC's in the past typically have been found to have a separatrix density 30% to 50% of the peak density at the magnetic null, and for that reason alone there was significant plasma transport across the separatrix onto the open field lines. Driving the density inward and keeping the density low at the separatrix effectively halts plasma loss and significantly enhances the FRC particle confinement. An analysis of the RMF FRC particle confinement was made,⁹ and the inferred particle confinement was indeed found to be much better than observed in even the largest FRC experiments performed previously, with a particle confinement time ~ 3 ms. This result was obtained with a confining magnetic field that was only 1/50th of that employed in the FRTP FRC experiments.

V. DISCUSSION

In order to reach conditions required for fusion, significant increases in plasma temperature must be achieved. As the confining field increases, so must the current drive and thus the plasma density and/or radius in order to support the increased field. Until the confinement scaling from the RMF experiments is known, it is not known by how much any of these quantities must be increased. It can be said, however, how the scaling of the field reversal ΔB should scale with electron temperature, radius and ω_{RMF} , and B_{RMF} based on past analysis.

For maximum current drive the RMF system should be operated with the minimum ratio of γ/λ required to maintain penetration at a radius sufficient to supply the necessary diamagnetic current. This ratio is of order one. From the internal field profile on STX, cosynchronous motion of the electrons is inferred for only a flux layer near the FRC edge that has a width d on the order of 3 cm. Assuming d to be the scale length of the region of RMF driven current, ΔB has the following dependence for $\gamma \sim \lambda$:

$$\Delta B(G) = 0.2B_{\text{RMF}}(G)T_e^{3/4}(\text{eV})d(\text{cm})\sqrt{\omega(10^6 \text{ s}^{-1})},$$

where a classical resistivity scaling for η was assumed. Given the scale length of the penetration, d , a larger magnetic field swing depends on an increase in electron temperature, as a large increase in the magnitude of the RMF field and frequency could pose a technological challenge. However, assuming a penetration no greater than that found on STX, for reactor electron temperatures ($T_e = 10^4$ eV), the field generated with STX RMF field parameters is 2.2 T. The plasma density from radial pressure balance ($T_e = T_i$) would be $3 \times 10^{20} \text{ m}^{-3}$. Classical particle confinement would require a plasma radius on the order of 1 m for fusion gain. If the RMF radial force provides even better confinement than assumed here, the FRC size could be reduced even further. Clearly though, more experimentation must be done to determine the confinement scaling and penetration effects of the RMF on the FRC at higher field and temperature.

ACKNOWLEDGMENTS

The authors would like to thank Dr. Richard Milroy, Dr. Alan Hoffman, and Dr. Samuel Cohen for many useful discussions, and Dr. Robert Brooks for data acquisition and analysis. The authors would also like to thank Daniel Lotz, Mark Kostora, and Jon Hayward for aid in the construction of the experiment. The work was supported by grants from NASA and the U.S. Dept. of Energy.

- ¹J. T. Slough, A. L. Hoffman, R. D. Milroy *et al.*, Phys. Plasmas **2**, 2286 (1995).
- ²J. Slough and K. Miller, "FRC Fusion Propulsion System for Deep Space Exploration," *35th AIAA/ASME/SAE/ASEE Joint Propulsion Conference*, Los Angeles, 1999 (American Institute of Aeronautics and Astronautics), Paper AIAA 99-2705 (to be published).
- ³A. L. Hoffman and J. T. Slough, Nucl. Fusion **33**, 23 (1993).
- ⁴H. A. Blevin and P. C. Thonemann, Nucl. Fusion Suppl. **1**, 55 (1962).
- ⁵A. J. Knight and I. R. Jones, Plasma Phys. Controlled Fusion **32**, 575 (1990).
- ⁶I. R. Jones, Phys. Plasmas **6**, 1950 (1999).
- ⁷R. D. Milroy, Phys. Plasmas **6**, 2771 (1999).
- ⁸W. N. Hugrass, Aust. J. Phys. **38**, 157 (1985).
- ⁹J. T. Slough and K. E. Miller, "Enhanced confinement and stability of a field reversed configuration driven by a rotating magnetic field," Phys. Rev. Lett. (submitted).
- ¹⁰G. Durance, G. R. Hogg, J. Tendys, and P. A. Watterson, Plasma Phys. Controlled Fusion **29**, 277 (1987).
- ¹¹W. N. Hugrass and R. C. Grimm, J. Plasma Phys. **26**, 455 (1981).
- ¹²G. A. Collins, G. Durance, and J. Tendys, J. Plasma Phys. **40**, 127 (1988).